MORPHOLOGICAL FILTERING OF SAR INTERFEROMETRIC IMAGES

S. Réjichi[(1)], F. Chaabane[(1)], F. Tupin[(2)], I. Bloch[(2)]

[(1)]URISA, École Supérieure des Communications de Tunis (SUP'COM), Tunisie.
[(2)]Institut TELECOM, TELECOM ParisTech, CNRS LTCI, France

ABSTRACT

This paper proposes a new morphological filter for SAR interferograms. It is based on a modified version of alternate sequential filters with reconstruction (MASF), in which the structuring elements are adaptively defined according to the fringe directions. This provides a good fidelity to the fringe information while efficiently removing noise. Another feature of the proposed approach is to apply the filter on the original interferogram and on shifted version, to overcome the wrapping of the phase, and to combine the two results. The proposed filtering technique is then tested on both simulated and real data with different levels of noise. It is also compared to previous techniques according to simplicity and noise reduction.

Index Terms— SAR interferometry, morphological filtering, alternate sequential filter, geodesic reconstruction.

1. INTRODUCTION

SAR and differential SAR interferometry are operational tools for monitoring surface deformation and topographic profile reconstruction. This technique is based on the fact that the phase difference between two different satellite position SAR signals is directly related to the elevation of a ground surface point. The major problems of SAR interferometry are the phase ambiguity and the temporal and geometric decorrelation [1]. First, as the phase information is included in $[0,2\pi]$, an unwrapping step is needed to correctly understand the interferometric data. Second, we are talking about geometric decorrelation when the angle of sight i.e. acquisition geometry changes between the two acquisitions dates. Then, SAR images are affected by temporal decorrelation when the considered surface inside the resolution element is changed due to long period cover. These effects are translated to an additional noise which is detrimental to the use of interferometric fringes. Particularly, these disturbances strongly compromise the phase unwrapping process thus the accuracy of the results i.e. the resulting Digital Elevation Model (DEM) or the deformation map. Therefore, a suitable method has to be used to improve the quality of the data. An appropriate filter should be applied on the complex interferometric data, before exploiting the phase. This procedure increases the signal to noise ratio of the phase field and decreases the number of residues.

In the literature, several methods have been proposed to reduce the interferometric phase noise [2] [3] [4] and some of them are based on basic mathematical morphology operators [5]. All these techniques, however, involve the loss of image details to a certain extent.

In this paper, we introduce a new morphological filter which is based on a modified alternate sequential filter. This filter is applied to the wrapped phase field and takes into account the properties of this type of images (fringes pattern). The performances of this filter are discussed and compared to other existing filters under different conditions. Both simulated and real data have been used for that purpose.

This paper is organized as follows. The proposed filtering method of SAR interferometric images is presented in Section 2. In Section 3 the obtained results on both simulated and real data with different levels of noise are discussed. Evaluation results are given for simulated images and the robustness of this filter is also tested by comparing it to other existing filters [2].

2. MORPHOLOGICAL FILTERING: ADAPTATION TO THE FRINGES PATTERN

In this section, we discuss a new strategy taking into account features which characterize the interferometric images i.e. the transition between the fringes and the value of each pixel which in fact reflects an altitude. This strategy estimates the direction of the gradient and includes it in the design of the structuring elements used in morphological filters. According to the method diagram (see Figure1), this section begins by presenting the interferogram shifting step. Secondly, the gradient estimation is explained. Thirdly, the principle of filtering taking into account the gradient direction is exposed. Finally, the recombination of filtered interferograms and the last filtering step are explained.
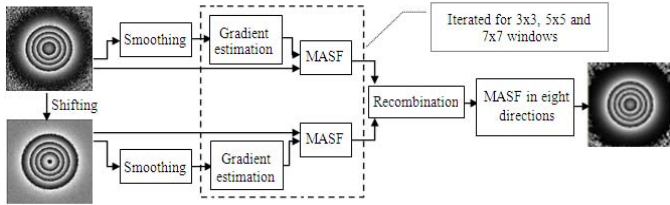
Figure 1. SAR interferometry morphological filter bloc diagram.

2.1. Interferogram shifting

This step consists in shifting the interferogram by π to have the most significant shifting (a pixel P located in the transition between two fringes will be in the middle of the next fringe and wrapped under its new position as shown in Figure 2). This idea will allow us to filter the same pixel P at two different positions on both interferograms as shown in Figure 2. Applying the shifting operation to the wrapped interferogram is an advantage since the unwrapping operation is an interferometric limitation. The next steps until recombination are performed on both original and shifted interferograms.
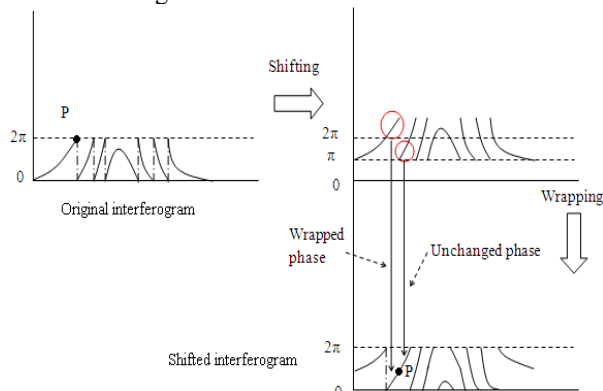
Figure 2. Interferogram shifting step.

2.2. Gradient estimation

2.2.1. Morphological smoothing
Since gradient estimation is highly sensitive to noise, a first smoothing step is applied before gradient computation. It is performed by using a sequential combination of morphological operators such as opening and closing operations [5]. This technique iterates openings and closings with different line structuring elements which are used in order to fit peak shapes in the interferogram. Thus, a set of segments are specified and this operation is repeated for all these segments.

In fact, it was noted that increasing the size of structuring elements for the same number of iterations does not improve the smoothing performance, in contrary, it alters the fringe system. For this reason, segments are defined in 3x3 window only (see Figure 3). Also, increasing the number of iterations does not improve the filter quality. Consequently, the

number of iterations is limited to three to optimize the algorithm computing time (see Figure 3).
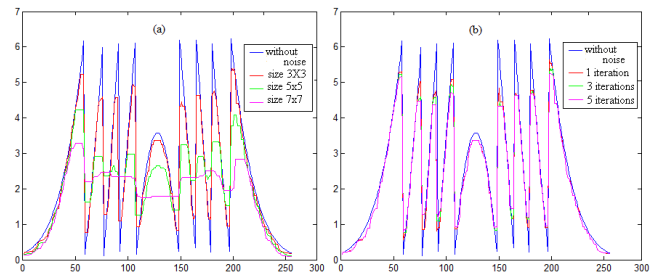
Figure 3. Interferoram profile after morphological smoothing. (a) Influence of the size of the segments. (b) Influence of the number of iterations.

2.2.2. Gradient estimation
This estimation is done by calculating, in a local neighborhood around each pixel, the modulus of the difference between the values of the central pixel and of its neighbors. The pixel that provides the minimum difference is selected. The direction orthogonal to the line formed by the central pixel and the selected one is considered as the gradient direction.

2.3. Morphological filtering

A modified version of the alternate sequential filter [5] is introduced in this paragraph. The filter relies on an alternate sequence of openings and closings with reconstruction, with increasing size of structuring elements, which are defined adaptively based on the gradient information previously computed.

The reconstruction steps allow to better preserve the fringe characteristics, in particular their level, which is of prime importance to reconstruct a proper altitude.

After each opening, a reconstruction by dilation is performed, thus recovering the levels in the preserved regions, while after each closing, a reconstruction by erosion is performed, preserving the transitions between the fringes.

The structuring element used in this work is orthogonal to the gradient direction estimated in the previous step, in order to preserve the fringe direction. The two structuring elements in nearest directions are also considered in order to provide more flexibility. This is done because the gradient direction may be misestimated and slightly shifted with respect to the real one. These directions are determined by the window size. For example, if the direction orthogonal to the gradient direction, on the 3x3 window, is vertical (cf. Figure 4) the nearest segments are the directions in black and blue (at 45 and 135 degrees respectively). When using several structuring elements, the supremum of the opening performed by each of them is computed (this is still an opening), and the infimum of the closings. Finally, one step of the filter can be expressed as:

$$f = R_E \left\{ \min_i \left[\phi_i(\rho(s)) \right], \rho(s) \right\} ; \rho(s) = R_D \left\{ \max_i \left[\gamma_i(s) \right], s \right\}$$

where s is the initial (noisy) image, γ_i the opening with the line structuring element i, R_D the reconstruction by dilation, R_E the reconstruction by erosion, ϕ_i the closing and f the filtered result.

It should be noted that the two steps of gradient estimation and morphological filtering are reiterated on 3x3, 5x5 and 7x7 windows.
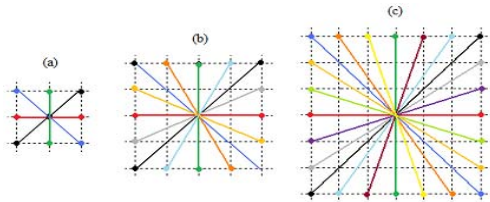
Figure 4. The line structuring elements in different directions depending on the chosen window size. (a) 3x3, (b) 5x5 and (c) 7x7 size.

2.4. Interferograms combination and final filtering

This step is performed by taking into account the neighborhood of each pixel. Indeed, the value of each pixel is compared to its 8-connected neighbors in the two images. A pixel value is chosen when it is the closest to the average of its neighbors. Of course, if the chosen value is that of the shifted interferogram, it must be returned to the original geometry. Thus, we build a new interferogram from the two filtered ones that contains the most homogenous values by selecting the pixel value approaching the fringes pattern i.e. gives the smoothest fringes.

Finally, because of geodesic reconstruction applied after each opening and closing operation, some noise may remain. Thus the proposed filter using line structuring elements in eight directions is applied again on the resulting interferogram to remove some residues.

3. RESULTS

The proposed filtering technique was tested on both simulated and real data with different levels of noise. Then it was evaluated for simulated images according to the Mean Squared Error (MSE), the Signal-to-Noise Ratio (SNR) and the Peak SNR (PSNR). First, images used for this work are presented. Then, results obtained on simulated and real data are shown and discussed. Finally, the robustness of this filter is also tested by comparing it to other existing filters [2].

3.1. Simulated and real data

In order to evaluate this new approach for interferoram filtering, a simulated interferogram was used. It was generated from a 2D Gaussian used as DEM (see Figure 5).

It is then wrapped according to parameters corresponding to the European satellite ERS1.

To simulate the noise affecting the interferometric fringes, we approximate the speckle model [6] by a colored noise, for the sake of precision [7]. It relies on a Gaussian white noise to generate the colored one. In general, the phase noise can be assimilated to a Gaussian one. In practice, two colored noises are generated for the two phase images, then the phase difference between these two noises is wrapped like the radar phase case (see Figure 5). Different noise levels are generated according to the correlation coefficient between the two noise signals: the higher the coefficient, the less noisy the signal. Also, a non homogenous coherence map is used to see the noise level discontinuity effects (see Figure 5). For real data, an ERS-1 interferogram covering the region of Bern is used (see Figure 6).
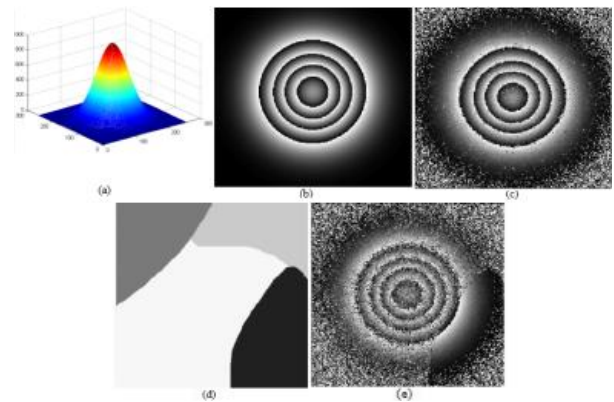
Figure 5. (a) Simulated DEM, (b) wrapped phase, (c) noisy interferogram, (d) non-homogenous coherence map, (e) noisy interferogram according to the coherence map.

3.2. Filtering results

In this paragraph, different filtering results are presented and some choices made for this approach are justified. First, as proved by Table 1, filtering in three directions, one orthogonal to the gradient and the two others in the nearest directions according to the window size (see paragraph 2.3), remarkably improves the results such as the MSE which decreases from 0.0764 for one structuring element to 0.0633 by adding the two nearest directions structuring elements (see Table 1).

Table 1. Filter performance evaluation according to the main steps.

	One structuring element	Three structuring elements	Recombination result	Final result
MSE	0.0764	0.0633	0.0274	0.0269
SNR	16.5126	17.2307	21.332	21.3616
PSNR	27.1353	27.1221	31.5782	31.6705

Also, Table 1 shows the contribution of the shifting step. The MSE in this case decreases from 0.0633 to 0.0274 after recombining the two interferograms. Finally, we note that the combination of the two filters (without and with shifting) slightly increases the interferogram quality by decreasing the MSE to 0.0269.

For the case of real interferograms, we can notice that the proposed filter removes the most significant noise present in the interferogram while preserving the fringes transitions (see Figure 6).
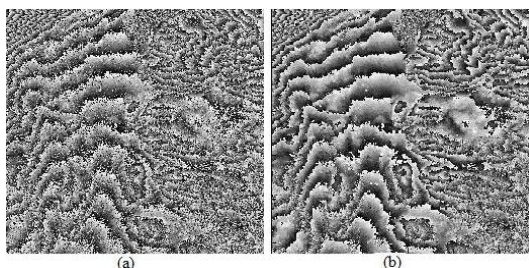
Figure 6. Real interferogram filtering. (a) Original interferogram. (b) Filtered interferogram.

3.3. Comparison

The proposed SAR morphological filtering approach is compared in this section to a more complex method developed in [2], based on the estimation of local frequency to find the best 2D sinusoid approximating locally the phase signal.
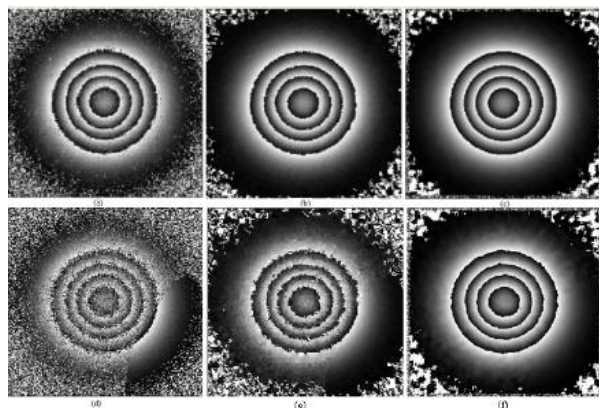
Figure 7. (a) Simulated noisy interferogram. (b) Result of the proposed method. (c) Result using the local frequency technique of [2]. (d) Simulated interferogram according to non-homogenous coherence map. (e) Result of the proposed method. (f) Result using the local frequency technique.

Table 2. Comparison study for simulated noisy interferogram.

	Simulated noisy interferogram		Simulated noisy interferogram according to coherence map	
	Proposed technique	Local frequency technique	Proposed technique	Local frequency technique
MSE	0.0269	0.0079	0.1675	0.0393
SNR	21.3616	26.9342	13.726	20.2578
PSNR	31.6705	36.9628	23.7229	30.0160

In the case of simple noisy interferogram, it is obvious that the proposed filter gives a good filtering result (MSE equal to 0.0269) by smoothing the fringes and preserving their transitions (see Figure 7(b)). Also, the local frequency technique has a lower error rate (MSE equal to 0.0079) than the proposed method due to its complexity and especially because this filter performs a multiscale processing. This is also shown for the simulated interferogram according to coherence map (see Figures 7(d), (e) and (f)). The local frequency technique enables to filter the interferogram with an acceptable visual result and an MSE equal to 0.0393 against 0.1675 for the proposed technique. Although it is not very robust to noise discontinuities, the proposed technique uses simple morphological tools, so it gains in simplicity compared to the local frequency technique with filtering results of sufficient quality for concrete applications.

4. CONCLUSION

In this paper, a new filtering technique based on morphological operators was introduced to reduce SAR interferometric noise. Steps of phase shifting and adapted line structuring elements based on gradient estimation have been introduced. Then, it was tested using simulated and real interferometric phase images. Satisfactory results are obtained when using homogeneous noise but this approach can still be improved in order to be robust according to noise discontinuities. A perspective for this work is to get rid of the phase ambiguity by applying the exponential to the phase and adapting morphological tools to the complex signal.

5. REFERENCES

[1] F. Chaabane, F. Tupin and H. Maître, "An empirical model for interferometric coherence", *SPIE Geosciences and Remote Sensing*, vol. 5980, pp. 59800-59800, September 2005, Belgique.

[2] E. Trouvé, J.M. Nicolas and H. Maître, "Improving phase unwrapping techniques by the use of local frequency estimates," *IEEE Trans. Geosci. and Remote Sensing*, 36(6), pp. 1963-1972, November 1998.

[3] J. Bioucas-Dias, V. Katkovnik, J. Astola, K. Egiazarian, "Absolute phase estimation: adaptive local denoising and global unwrapping", *Applied Optics*, pp. 5358-5369, 2008.

[4] A.B. Suksmono, A. Hirose, "InSAR image restoration by using stochastic complex-valued neural network", *IEEE Trans, Geosci. and Remote Sensing*, pp. 699-709, 2002.

[5] P. Soille, "*Morphological Image Analysis*", Springer-Verlag, 2003.

[6] H. Maître, "*Processing of Synthetic Aperture Radar Images*", Wiley-ISTE, 2008.

[7] R. Bamler and P. Hartl, "Synthetic Aperture Radar Interferometry", *Inverse Problem*, vol. 14, 1998.